ARTICLES

First-Principles Calculation of the ^{17}O NMR Parameters of a Calcium Aluminosilicate Glass

Magali Benoit*

CEMES, 29 rue Jeanne Marvig, BP 94347, 31055 Toulouse Cedex 4, France

Mickaël Profeta and Francesco Mauri

Laboratoire de Minéralogie-Cristallographie de Paris, Université Pierre et Marie Curie, 4, place Jussieu, 75252 Paris Cedex, France

Chris J. Pickard

TCM Group, Cavendish Laboratory, Madingley Road, Cambridge, CB3 OHE, United Kingdom

Mark E. Tuckerman

Department of Chemistry and Courant Institute of Mathematical Sciences, 100 Washington Square East, New York University, New York, New York 10003

Received: February 18, 2004; In Final Form: February 9, 2005

We have computed the ^{17}O NMR parameters of an amorphous calcium aluminosilicate (CAS) from first-principles. The atomic coordinates of a CAS glass of composition $(CaO)_{0.21}(Al_2O_3)_{0.12}(SiO_2)_{0.67}$ were obtained by quenching a liquid to room temperature by the means of ab initio molecular-dynamics simulations of the Car−Parrinello type. The structure of the glass is found to be overall in good agreement with diffraction experiments. Some excess nonbridging O (NBO) atoms are found and are compensated by tricluster O atoms, i.e., by 3-fold coordinated O atoms to 4-fold coordinated Al or Si atoms. The glass coordinates were used to compute the ^{17}O NMR parameters using GGA-DFT and a correction of the Ca 3d orbital energy. The chemical shifts and the electric field gradients were obtained with the gauge including projector augmented-wave (GIPAW) and the projector augmented-wave (PAW) methods, respectively. The simulated 2D-3QMAS NMR spectrum of the CAS glass is in very good agreement with the available experimental data, notably because it takes into account the disorder present in the glass. This agreement further validates our CAS glass model. We show that the oxygen triclusters are not visible in a 2D-3QMAS NMR ^{17}O spectrum since their NMR parameters overlap with those of the Al−O−Si, Si−O−Si, or Al−O−Al sites. Finally, correlations between the structural characteristics and the values of the NMR parameters are extracted from the calculation with the aim of helping the interpretation of NMR spectra of glasses of similar compositions.

1. Introduction

Aluminosilicate glasses and melts are essential to a wide range of fundamental and applied scientific disciplines, including the glass industry, nuclear waste confinement, petrology, ceramics, and geology. The thermodynamical properties of these materials are mainly determined by their composition.[1] When introducing Al_2O_3 in the fully connected corner-sharing tetrahedral network of amorphous silicates, the Al atoms substitute for the Si atoms in the center of the tetrahedra thus leading to charged $(AlO_4)^-$ units. The positive charges of cations such as $M = Na^+$, Ca^{2+}, K^+ etc. can then compensate for the charge of the $(AlO_4)^-$ units and the Al and Si atoms are thus maintained in the center of tetrahedra, connected by shared corners. The cations are called *charge-balance ions*, and the viscosity of the melt at the same T_g/T (i.e., the inverse temperature normalized by the glass transition temperature) should reach a maximum for a total compensation of charges by the cations, e.g. for $M = Ca^{2+}$ the system is fully polymerized at a ratio $R = [CaO]/[Al_2O_3] = 1$. Only if the concentration of cations becomes larger than what is needed for a full compensation of the $(AlO_4)^-$ units (for a ratio $R > 1$) is the corner-sharing tetrahedral network broken: some Si−O or Al−O bonds are replaced by weak M−O bonds, and the cations are then called *modifiers* (for a review, see ref 2). The O atoms participating in these Si−O−M and Al−O−M linkages are named nonbridging O (NBO), and their proportion in a material is known to play a crucial role in its thermodynamic properties.

* Corresponding author: mbenoit@cemes.fr.

10.1021/jp0492570 CCC: $30.25
Published on Web 03/15/2005

However, experiments have shown that this picture is not entirely correct for some aluminosilicate systems. Indeed the viscosity at the same T_g/T for sodium and calcium aluminosilicate melts, at high silica content, is not maximum for $R = 1$ but for R slightly lower than one.[3] This may indicate that the network at $R = 1$ is not fully polymerized and that NBOs exist in the system. To preserve the total number of Al−O and Si−O bonds, the presence of NBO should be compensated by highly coordinated O sites, for example, O triclusters. Here we define the O triclusters to be O bonded to three Al and/or Si atoms that are 4-fold coordinated. Notice that, here, we do not consider as triclusters the oxygen atoms bonded to 5-fold and 6-fold coordinated Al sites, as is done in previous work (see, e.g., ref. 4). Yet because of the lack of positional order, the experimental detection of such local structural units remains a challenging problem. Only very local probes such as X-ray absorption or NMR spectroscopies can help one to discriminate between the different structural units that might be present in very small proportions.[5−15] Recently, ^{17}O NMR 3QMAS spectroscopy has been performed on a calcium aluminosilicate glass of tectosilicate composition ($R = 1$) with the aim of clarifying some of these open questions.[6,7] The 3QMAS spectrum showed a well-defined additional peak that was clearly attributed to the presence of NBO atoms in the system. A weaker peak (the D peak) in the 3QMAS spectrum has been tentatively assigned to O triclusters. Unfortunately, the interpretation of a NMR spectrum for a complex glass is extremely difficult and, although important insights have been obtained from this experimental technique,[6,9] the positional disorder prevents unique assignment of the different O sites from their ^{17}O NMR response. For this reason, it would be of great interest to have a way of reliably computing the NMR response of a model system for which we precisely control all atomic positions.

Calculations of NMR parameters in calcium aluminosilicate systems have been performed previously using small clusters to represent the local environment.[16,17] Given the small size of the clusters, these calculations were not able to represent the disorder present in ternary glasses. In addition the use of clusters introduces finite-size errors that are difficult to control and to estimate.[16,17] Recently the accurate calculation of the NMR parameters in extended solids has become possible using periodic boundary conditions. The chemical shifts and the electric field gradients can be obtained from first principles with the gauge including projector augmented-wave (GIPAW)[18] and the projector augmented-wave (PAW) methods,[19,20] respectively. Reference 21 proved the high accuracy of these methods for the prediction of the ^{17}O NMR parameters in calcium-aluminosilicate crystalline reference compounds. This accuracy was used to assign the experimental ^{17}O NMR spectra of grossite ($CaAl_4O_7$)[22] and wollastonite ($CaSiO_3$).[23]

In this work, we generated a calcium aluminosilicate glass quenched from the melt using ab initio molecular-dynamics simulations of the Car−Parrinello type.[24] We compared the calculated NMR parameters obtained from the glass local structure to experimental NMR spectra by computing the ^{17}O 2D-3QMAS NMR spectrum from first-principles using the GIPAW and PAW methods. The use of the molecular-dynamics-generated model and of periodic boundary conditions allowed us to consider the effect of disorder in the simulation of the NMR spectra. Correlations between the structural units and the values of the NMR parameters are extracted from the calculation with the aim of aiding in the interpretation of NMR spectra of glasses of similar compositions.

In section 2, we present the details of the Car−Parrinello molecular-dynamics simulation and the resulting structural properties of the glass sample. In section 3, the details of the NMR calculations are given and the NMR results are presented and compared to experiments. Finally, we discuss the results and present conclusions.

2. Structural Properties of the CAS Glass Sample

In this section, we give the technical details of the Car−Parrinello molecular-dynamics simulation performed in order to generate the glass sample. We then analyze the structural characteristics of the glass thus obtained.

2.1. Generation of the Glass Sample. A calcium aluminosilicate system containing 100 atoms (22 Si, 8 Al, 63 O, and 7 Ca) in a cubic box of edge length of 11.36 Å was equilibrated at 3000 K over 6.8 ps (for the simulation details of the liquid equilibration, see ref 25). At this very high temperature, the mean square displacements exhibit a diffusive behavior and the Si atoms (which diffuse least) have diffused by at least one Si−O bond length. With these two conditions fulfilled, the CAS liquid was well equilibrated, and the final configuration of the liquid did not reflect the initial configuration. The composition of the system was chosen in order to be close to the composition of the French nuclear waste confinement glasses and is equal to 67 mol % SiO_2, 12 mol % Al_2O_3, and 21 mol % CaO. For this composition, the tetrahedral network is not fully polymerized and the stoichiometry gives a number of nonbridging O atoms equal to 6, if no other defective structural units (such as highly coordinated Si, Al or O atoms) are present.

At the end of the equilibration simulation, we quenched the system linearly from 3000 to 300 K with a quench rate of 3.6×10^{14} K/s; i.e., the velocities of all atoms at each time step were reduced by a constant factor. We then let the system relax at 300 K over an additional 2 ps simulation. These simulations were carried out using the CPMD software[26] within the framework of density functional theory (DFT)[27] using the generalized gradient approximation. Specifically, the B-LYP functional[28,29] was employed. The electronic wave functions were expanded in plane waves at the Γ point of the Brillouin zone up to an energy cutoff of 70 Ry. The core electrons were replaced by norm-conserving pseudopotentials of the Trouiller−Martins type for O[30] and of the Gödecker type for Si, Al, and Ca.[31] For the Car−Parrinello dynamics, a fictitious electronic time scale parameter of $\mu = 800$ au and a time step of 5 au were used. During the quench, because of a very small electronic gap, Nosé-Hoover thermostat chains were applied on the electronic degrees of freedom.[32,33] The small gap comes from the combination of two facts: (i) the DFT calculations always underestimate the value of the gap and (ii) in silicates, the gap decreases with increasing temperature. At 300 K, no thermostats were used.

At this point, we let the simulation cell relax in order to minimize the internal stress. This was done using a plane-wave energy cutoff of 120 Ry which appeared to be necessary in order to obtain a good convergence of the pressure. The system was found to have a zero stress for a density of 2.42 g/cm^3 which appears to be too low compared to the experimental density of glasses of similar compositions (2.55−2.60 g/cm^3).[1,34] This fact has already been attributed, both experimentally and theoretically, to the use of a very high quench rate to generate the glass.[35] Finally we let the system relax at the new volume over an additional 2 ps simulation.

2.2. Structure of the CAS Glass. In this section, we analyze the structural characteristics of the CAS glass sample. In Figures

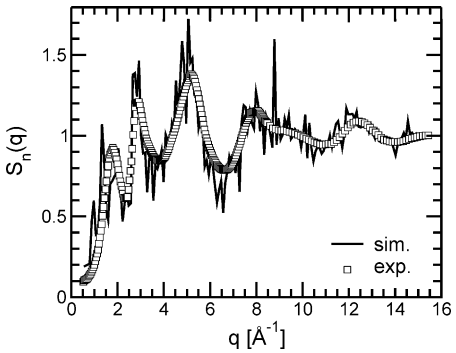

Figure 1. Comparison of the experimental neutron structure factor of a glass of composition 60% SiO_2−10% Al_2O_3−30% CaO (from ref 37) and the calculated neutron structure factor. The scattering lengths were taken to be equal to $b_{Si,O,Al,Ca}$ = 4.149, 5.803, 3.449, 4.700 fm.

1, 2, 3, 4, and 6, the results presented were obtained by averaging over the final 1.6 ps of simulation at 300 K. In all other figures, the structural results were obtained from the final atomic positions quenched to 0 K.

To compare the global structure of the model glass with the one of real systems, we computed the neutron static structure factor. This was done using the relations:

$$S_n(q) = \frac{1}{\sum_{\alpha} N_\alpha b_\alpha^{\,2}} \sum_{\alpha\beta} b_\alpha b_\beta S_{\alpha\beta}(q) \qquad (1)$$

with

$$S_{\alpha\beta}(q) = \frac{f_{\alpha\beta}}{N} \sum_{l=1}^{N_\alpha} \sum_{m=1}^{N_\beta} \langle \exp(i\mathbf{q}\cdot(\mathbf{r}_l - \mathbf{r}_m)) \rangle \qquad (2)$$

where **q** is the scattering vector, N the number of atoms, and N_α and N_β the number of atoms of species α and β, respectively. The factor $f_{\alpha\beta}$ is equal to 0.5 for $\alpha \neq \beta$ and equal to 1.0 for $\alpha = \beta$, b_α and b_β are the neutron scattering lengths of species α and β, and are equal to 4.149, 5.803, 3.449, 4.700 fm for Si, O, Al and Ca, respectively.[36] Since no experimental data were available for the specific composition of the present work, we compare our structure factor with an experimental one measured for a glass of composition 60% SiO_2, 10% Al_2O_3, and 30% CaO. The comparison between the computed and experimental structure factors from ref 37 is presented in Figure 1. The agreement is good both for the positions of the peaks and for their intensities. The difference between the two compositions (the SiO_2/CaO ratio) should only affect the relative intensities of the first two peaks and, within the errors due the statistics of the calculated structure factor, the obtained agreement gives us confidence in the simulated glass structure.

In Figure 2, the pair correlation functions (PCF) involving the network forming atoms (Si, Al and O) are presented. From the Si−O and Al−O PCFs (Figure 2, parts b and d), it is clear that the Si and Al atoms sit in the center of O tetrahedra. The integrated coordination numbers show a well-defined plateau at a value of 4, which indicates that the Si and Al atoms have an average coordination of 4. A more detailed analysis revealed that all Si atoms have indeed a coordination of 4 whereas one of the Al atoms has a fifth O neighbor which is located at a larger distance than the other four (∼ 2.37 Å). The first peak maxima positions give the most probable distances for Si−O at ∼1.63 Å and for Al−O at ∼1.74 Å, in very good agreement

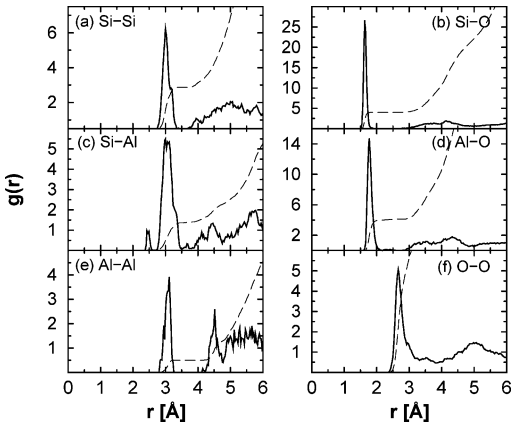

Figure 2. Pair correlation functions (bold lines) involving the network atoms (Si, Al and O) of the CAS glass at 300 K. The dashed lines are the integrated coordination numbers.

with experimental distances measured in aluminosilicate glasses and crystalline analogous of different compositions.[5,40−46]

The positions of the first minima after the first peaks in the Si−O and Al−O PCFs give the cutoff radii of the coordination spheres of the Si and Al atoms. These were estimated to be 2.00 and 2.17 Å, respectively. These cutoff radii were then used to determine the coordination numbers of the O atoms in the system. Hence, among the 63 O atoms, eight are nonbridging O and two are O atoms forming triclusters (one $OAlSi_2$ and one OAl_2Si). Given the composition of our glass sample, there are two NBO atoms "in excess" of the simple stoichiometric prediction, which are compensated by the presence of the two triclusters. This result tends to confirm the hypothesis proposed by the authors of refs 6 and 7 and is consistent with the tendency observed in the melt.[25] From this analysis, we also found out that all the NBO atoms are bonded to Si atoms and none to Al atoms, which is in agreement with the experimental results obtained from energy-dispersive X-ray diffraction.[45,46] As a consequence, all aluminum atoms are found in a Q^4 environment (all O neighbors are bridging) whereas one Si atom (4.5%) is found in a Q^2 environment (two of the four O neighbors are nonbridging) and six Si atoms (27.3%) in a Q^3 environment (one of the four O neighbors is nonbridging).

The PCFs between the network forming atoms (Si and Al) can give information on the connections between the tetrahedra (Figure 2, parts a, c, and e). It is interesting to note that there is a main first peak at ∼ 3 Å for Si−Si, Si−Al, and Al−Al, which shows that there are Si−O−Si, Si−O−Al, and Al−O−Al linkages in the system (only one Al−O−Al is found). This result is in agreement with recent experimental and theoretical findings which support the fact that the so-called Al avoidance principle, confirmed in most of the aluminosilicate crystals, does not necessarily hold in their glassy counterparts.[9,14,16,47−51] In the present glass sample, the two Al atoms participating to the Al−O−Al linkage are both connected to the same tricluster O atom. In Figure 2c, one can distinguish a small pre-peak before the first peak of the Si−Al PCF. This pre-peak corresponds to a Si tetrahedron and an Al tetrahedron that share a common edge. This structural unit should not be present in the glass and is certainly due to the very high quench rate and the small system size used to generate the glass sample. However, one should notice that the percentage of this type of defects is very low (3.33%) and should affect the glass structure only locally since it is not a coordination defect.

In Figure 3, the PCFs involving the Ca atoms are shown. The figure shows that there is a well-defined first peak in the

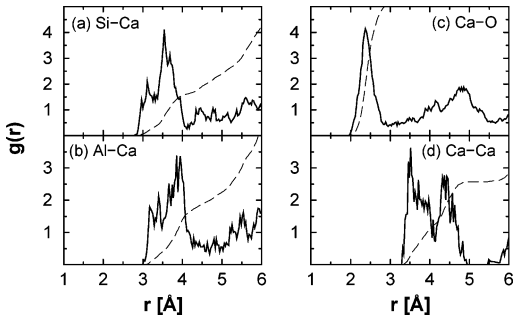

Figure 3. Pair correlation functions (bold lines) involving the Ca atoms of the CAS glass at 300 K. The dashed lines are the integrated coordination numbers.

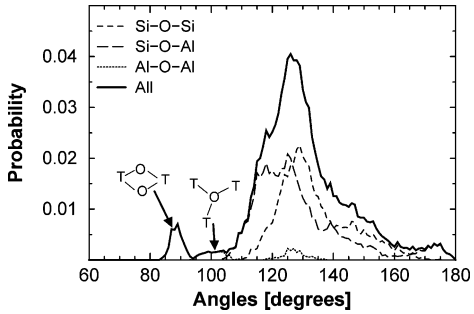

Figure 4. Inter-tetrahedral angle distributions in the CAS glass at 300 K: total distribution (bold line), Si−O−Si distribution (short-dashed line), Si−O−Al distribution (long-dashed line) and Al−O−Al distribution (dotted line).

Ca−O PCF (Figure 3c) with an average coordination number of ∼5. This coordination number seems to be smaller than the coordinations of ∼6 or ∼7 measured in CAS glasses.[41,43] From the position of the first peak maximum, we deduce a most probable Ca−O distance of ∼2.36 Å. This value is slightly too small compared to experimental results published in[43] where Ca−O varies between 2.40 and 2.64 Å but appears to be in much better agreement with other experimental measurements that give a distance between 2.3 and 2.5 Å.[41,46,52] The Si−Ca and Al−Ca PCFs (Figure 3, parts a and b) show broader but still well-defined first peaks, illustrating the fact that correlations between the Ca atoms and the network former atoms are similar independent of whether the Ca atoms have a compensating or a modifying character. Finally, it is difficult to draw conclusions from the Ca−Ca PCF since the correlations occur on a longer length scale, close to half of the simulation cell.

The angle distributions have been evaluated at 300 K for the network forming atoms only. The results are presented in Figure 4 for the T−O−T angles (T = Si, Al) and in Figure 6 for the O−T−O angles. The total T−O−T distribution is quite broad and exhibits a central peak at ∼ 128°, a long tail toward 180° and two small peaks at ∼90° and ∼105°. A detailed analysis reveals that the smaller angles can be attributed to the anglular values found in the tricluster units and between the edge-sharing tetrahedra. From a decomposition of the distribution in separate Si−O−Si, Si−O−Al, and Al−O−Al contributions, the Si−O−Al angles appear to be responsible for the shift of the distribution to lower values, when compared to the angle distribution of pure silica.[35,53−55] However the Si−O−Si distribution is also slightly shifted to lower values compared to that of pure silica, a fact that is most likely due to the high quench rate used to generate the glass sample.[35,56]

On the contrary, the effect of the density on the T−O−T angle distribution should not be very large. In a recent study,[57] the variation of the T−O−T angles as a function of the density

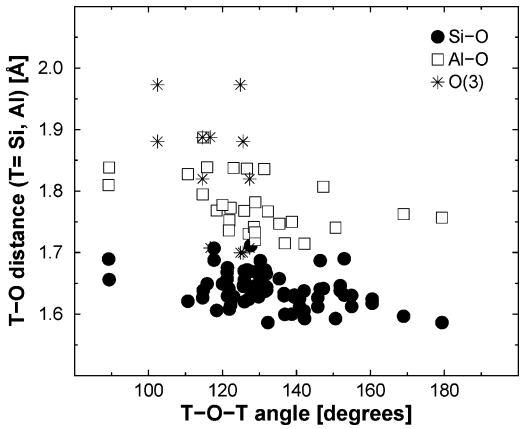

Figure 5. T−O bond lengths as a function of the corresponding T−O−T angles in the amorphous CAS sample at 0 K, with empty squares for T = Al, filled circles for T = Si, and stars for the O triclusters.

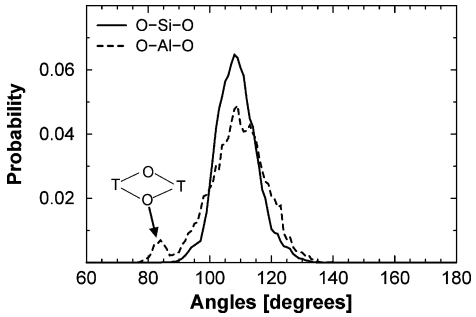

Figure 6. Intratetrahedral O−Si−O (bold line) and O−Al−O (dashed line) angle distributions.

has been monitored in amorphous silica using ab initio molecular-dynamics simulations. In this work, the maximum of the Si−O−Si angle distribution was shifted by 10° for a density change from 2.20 g·cm^{-3} to 2.45 g·cm^{-3} (≈10%). If we assume that the variation would be similar in the CAS glass, then the effect of the too low density of our model with respect to experiment (≈4%) on the T−O−T angle would affect the results only slightly since the T−O−T angles vary between 110 and 180° (see Figure 4).

In previous work,[42,43] a correlation between the T−O−T angles and the length of the T−O bonds has been sought for silicate glasses, either from a compilation of experimental data measured on several crystalline analogues or from static ab initio calculations on small clusters. In an attempt to look for a correlation of this type in our sample, we computed the T−O distances at 0 K associated with the corresponding T−O−T angles and plotted the results as black circles for the O atoms in Si−O and as empty squares for the O atoms in Al−O in Figure 5. The O triclusters (O_3) are depicted as stars and give rise to three different angles and T−O distances. In general the variation of the Si−O bond length is quite small compared to the Al−O bond lengths, in good agreement with ab initio studies of the potential energy surface of the $H_6Si_2O_7$ molecule.[42] Note that the O atoms involved in a tricluster unit give rise to small angles and large distances. The points at 90° correspond to the edge-sharing tetrahedra.

In Figure 6, the intra-tetrahedral angle distributions are depicted for the O−Si−O and the O−Al−O angles, separately. The O−Si−O angle distribution is peaked at ∼109° ± 7, which is very close to the value of the ideal tetrahedral angle. The O−Al−O angle distribution is noisier and even if the main peak is located at the same value of 109°, there are smaller peaks

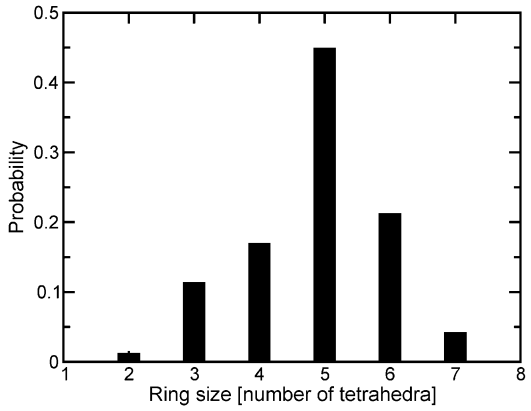

Figure 7. Distribution of the rings size.

between 70 and 90° that correspond to nonideal tetrahedral arrangements. Indeed a detailed analysis revealed that these small peaks are due to the edge-sharing tetrahedra.

The distribution of the rings size, i.e., the number of connected Si/Al tetrahedra, i.e., the number of closed Si/Al−O loops, has been evaluated and is shown in Figure 7. The distribution is maximum for the five-membered rings and ranges from two- to seven-membered rings. The distribution is very similar to that of the $Al_2O_3-SiO_2$ glass model[58] and, compared to that of pure silica, it is slightly shifted toward smaller sizes.[35] This shift could be due to the high quench rate used to generate the glass, since it has been shown for silica that the distribution of the ring size shifts toward smaller sizes with increasing quench rate.[35]

Finally, concerning the possible finite size effects, in a recent classical molecular-dynamics study,[38] we have shown that (i) finite size effects exist for CAS glasses containing less than 200 atoms and (ii) these size effects depend very much on the type of potential that is used. Moreover we have shown that the effects of the system size on the local structure disappear—even in a system containing 100 atoms—when the structure is refined using ab initio MD.[39] Therefore, we do not think that size effects influence the *local* structure of the glass in the present case.

3. First Principles Calculations of the ^{17}O NMR Parameters and 3QMAS Spectrum

To check the validity of our model glass, it is necessary to compare its structural characteristics with experimental data. However, it is extremely difficult to obtain detailed information on the structure of such complex glasses. Solid-state NMR is one of the few tools which can probe the local structure of such systems and from which valuable information can be extracted. For this reason, the first-principles calculation of the ^{17}O NMR response of our glass sample appears to be necessary in order to validate our model. At the same time, this approach can be extremely useful in helping to interpret the NMR spectra, which can be quite challenging in the case of ^{17}O.

In this section, we first present the details of the NMR response calculations, and then the results obtained for the NMR parameters and the 2D-3QMAS spectrum for the CAS glass sample.

3.1. Details of the NMR Response Calculation. An applied external magnetic field **B** induces a nonuniform magnetic field $\mathbf{B}_{in}(\mathbf{r})$ within the sample. The NMR shielding tensor, $\vec{\sigma}(\mathbf{r})$ is defined as $\mathbf{B}_{in}(\mathbf{r}) = \vec{\sigma}(\mathbf{r})\mathbf{B}$. The isotropic shielding $\sigma(\mathbf{r})$ is one-third of the trace of the shielding tensor and the isotropic chemical shift $\delta(\mathbf{r})$ for a nucleus in the position **r** is defined as

$$\delta(\mathbf{r}) = -[\sigma(\mathbf{r}) - \sigma^{\mathrm{ref}}] \tag{3}$$

where σ^{ref} is the isotropic shielding of the same nucleus in a reference system. For ^{17}O the reference is a spherical liquid water sample. Nuclei with a spin larger than $^1/_2$ have quadrupolar parameters related to the traceless electric field gradient (EFG) $\bar{G}(\mathbf{r})$,

$$G_{\alpha\beta}(\mathbf{r}) = \frac{\partial E_\alpha(\mathbf{r})}{\partial r_\beta} - \frac{1}{3}\delta_{\alpha\beta}\sum_\gamma \frac{\partial E_\gamma(\mathbf{r})}{\partial r_\gamma} \tag{4}$$

where α,β,γ denote the Cartesian coordinates x, y, z and $E_\alpha(\mathbf{r})$ is the local electric field at position **r**. If we label the eigenvalues of the EFG tensor V_{xx},V_{yy},V_{zz} so that $|V_{zz}| > |V_{yy}| > |V_{xx}|$, then one can define the quadrupolar coupling as

$$Cq = \frac{eQV_{zz}}{h} \tag{5}$$

and the asymmetry parameter as

$$\eta = \frac{V_{xx} - V_{yy}}{V_{zz}} \tag{6}$$

where e is the absolute value of the electron charge, h is the Planck constant, and Q is the nuclear quadrupolar momentum. Finally, the constant P_q is equal to $Cq\sqrt{1+\eta^2/3}$.

In our calculation, we obtain absolute shielding tensor. To fix the ^{17}O relative chemical shift scale we used the value of 261.6 ppm for σ^{ref} that has been obtained in ref 19, by comparing the experimental and theoretical ^{17}O relative chemical shifts of SiO_2 crystalline systems. To compute Cq, we used the experimental quadrupolar momentum $Q = 2.5510^{-30}$ m^2.

The calculations were performed within density functional theory (DFT). The core-valence interactions were described by Trouiller−Martin norm conserving pseudopotentials[59] in the Kleinman−Bylander[60] form, with s nonlocality for O, and s and p nonlocality for Si, Al and Ca. The core part for O is $1s^2$ and for Si, Al and Ca is $1s^22s^22p$.[6] The core radius is 2.0 au for Si, Al, and Ca and 1.45 au for O and 1.40 au for the s channel. The structure was described as an infinite periodic solid using periodic boundary conditions. The orbitals were expanded in a plane wave basis with a cutoff of 80 Ry. The integral over the Brillouin zone was done using the Baldereschi ($^1/_4$, $^1/_4$, $^1/_4$) special k-point.[61]

To compute the shielding tensor using pseudopotentials we used the GIPAW[18] approach. This permits the reproduction of the results of a fully converged all-electron calculation. To compute the EFG tensor, we used a PAW approach to reconstruct the all-electron calculation.[19,20,62] For PAW and GIPAW calculations, we used two projectors in each s, p, and d angular momentum channel. This approach has been successfully applied to the calculation of the ^{17}O parameters in SiO_2 polymorphs and zeolites.[19]

We used the generalized gradient approximation of DFT developed by Perdew, Burke and Ernzerhof (PBE)[63] which gives results very similar to those obtained with the so-called PW91[64] and corrects some numerical instabilities. In a previous publication,[21] it was shown that ^{17}O chemical shifts are very sensitive to the hybridization between the O 2p orbitals and the 3d orbitals of neighboring Ca atoms. In the PBE approximation, the energy of Ca 3d orbitals is too low and the hybridization with O 2p

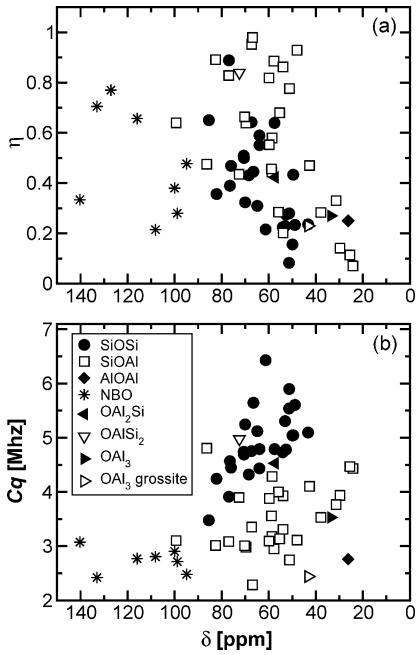

Figure 8. (a) Asymmetry parameter η and (b) quadrupolar coupling Cq as a function of the chemical shift in the CAS glass with different symbols for the different O sites. The OAl_3 site of the grossite crystal has been added for comparison.

orbitals is overestimated. As a consequence, the ^{17}O chemical shift computed with PBE are affected by very large errors (up to 124 ppm) for the O sites close to Ca atoms. As shown in ref 21, the DFT-PBE error can be efficiently corrected by shifting by a constant value of +3.2 eV, the position of the Ca 3d orbitals in the pseudopotential generation. This shift is found to be transferable to very different Ca and O environments. The ^{17}O NMR parameters predicted with the modified Ca pseudopotential[21] are very accurate and allowed the assignment of the experimental ^{17}O NMR spectra of grossite ($CaAl_4O_7$)[22] and wollastonite ($CaSiO_3$)[23] crystals. Thus, for the present calculations we followed ref 21, by using a modified Ca pseudopotential with shifted 3d orbitals.

Finally, to correct the systematic errors on the Si−O and Si−Al distances produced by the DFT functional used for the NMR calculations, we decreased the supercell lattice vector by 1.4%.

3.2. ^{17}O Parameters for the CAS Glass: NBO, Si−O−Si, and Si−O−Al Sites. In Figure 8, the computed asymmetry parameters η (a) and quadrupolar coupling Cq (b) are represented as a function of the chemical shift δ for all ^{17}O sites in the CAS glass. The different types of O sites (NBO, Si−O−Si, and Si−O−Al) occupy well-defined regions of the (Cq, δ) space (Figure 8b). For the Si−O−Si and Si−O−Al sites, a weak correlation between Cq and δ and between η and δ is observable.

We reproduced the 2D-3QMAS spectrum using Stebbins's convention.[65] In a 2D-3QMAS spectrum, each ^{17}O site gives rise to a sharp resonance in the δ_{3Qiso} dimension at the position:

$$\delta_{3Qiso} = -\frac{17}{31}\delta - \frac{3}{1550}\frac{P_q^2}{\nu_0^2} \quad (7)$$

and a broad MAS spectrum in the MAS dimension. The center of mass of the MAS spectrum is given by

$$\delta^{MAS} = \delta - \frac{3}{500}\frac{P_q^2}{\nu_0^2} \quad (8)$$

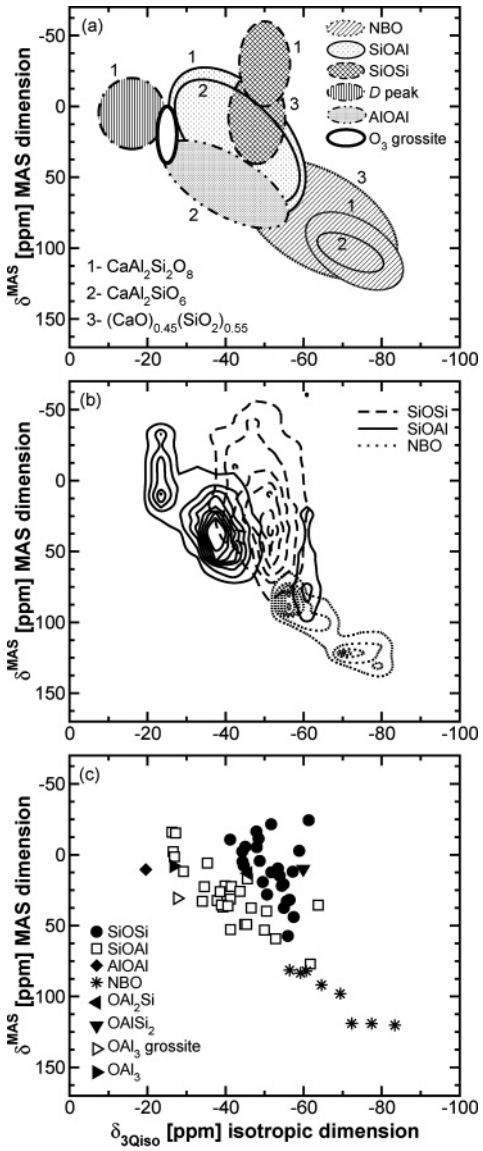

Figure 9. ^{17}O NMR 3QMAS spectra for a magnetic field of 9.4 T computed from the coordinates of the CAS sample. In panel (c), the computed δ^{MAS} as a function of δ_{Qiso} are presented using different symbols for the different O sites. Panel (b) represents the simulated 2D spectra as contour plots for the SiOSi, SiOAl and NBO sites, and panel (a) shows a compilation of experimental data for CAS glasses of different compositions: (1) $CaAl_2Si_2O_8$,[6] (2) $CaAl_2O_4$,[9] and (3) $(CaO)_{0.45}(SiO_2)_{0.55}$[66] as well as the grossite O_3 site from.[9] The position of the main peaks are schematically represented by ellipsoids.

where ν_0 is the spectrometer frequency, $\nu_0 = 54.2$ MHz for a 9.4 T spectrometer.

In Figure 9c, we present the computed δ^{MAS} as a function of δ_{3Qiso} for a magnetic field of 9.4 T using different symbols for the different types of O sites. In Figure 9b, we present a simulated 2D spectra as a contour plot for the NBO, the Si−O−Si, and the Al−O−Si sites. In this case, for each O site we used the computed NMR parameters to obtain a MAS spectra in the MAS dimension and a sharp distribution in the isotropic dimension centered at δ_{3Qiso}. The contributions of all sites were summed and a 65 Hz Gaussian broadening was applied in both dimensions. Figure 9a represents schematically the peak positions of experimental data measured in glasses of different compositions.[6,9,66]

The comparison of the simulated NMR spectra for the of the NBO, the Si−O−Si, and the Al−O−Si with the ^{17}O 2D-3QMAS NMR spectra measured on calcium aluminosilicate

TABLE 1: Structural Information (T−O−T Angles and T−O Bond Lengths; T = Si, O) and ^{17}O NMR Parameters for the Different Triclusters in the CAS Glass and in the Grossite Crystal from Reference 21

site	δ	Cq	η	δ_{3Qiso}	δ^{MAS}	angle (deg)		length (Å)	
OAl_3 grossite	43.18	2.44	0.23	−27.53	30.39	Al−O−Al	122.3	O−Al	1.80
						Al−O−Al	122.8	O−Al	1.79
						Al−O−Al	109.1	O−Al	1.78
OAl_3 CAS	33.59	3.53	0.27	−26.50	8.53	Al−O−Al	126.5	O−Al	1.86
						Al−O−Al	123.0	O−Al	1.81
						Al−O−Al	105.1	O−Al	1.79
OAl_2Si CAS	57.36	4.53	0.42	−45.79	12.99	Al−O−Al	102.4	O−Al	1.95
						Al−O−Si	125.6	O−Al	1.85
						Al−O−Si	124.9	O−Si	1.68
$OAlSi_2$ CAS	72.49	4.97	0.84	−59.90	10.09	Al−O−Si	116.8	O−Al	1.86
						Al−O−Si	114.6	O−Si	1.79
						Si−O−Si	127.4	O−Si	1.68

glass systems[6,7,9,66] shows excellent agreement. In particular our approach is able to reproduce not only the average values of the NMR parameters for each type of site, but also the shape of the distributions of the NMR parameters given by the disorder. The agreement between the experimental and calculated spectra validates the structure of our model glass.

3.3. ^{17}O Parameters for the CAS Glass: O Triclusters. In our model calcium aluminosilicate glass, the excess number of nonbridging O is compensated by the existence of O triclusters. It is interesting to check whether these O triclusters can be detected by ^{17}O NMR spectroscopy. Our glass model contains only one OAl_2Si and one $OAlSi_2$ site. To obtain an OAl_3 tricluster site in the glass environment, we exchanged the Si atom of the $OAlSi_2$ tricluster successively with all the other Al atoms in the sample and relaxed the structure. Then we chose the Si−Al exchange that gave the lowest total energy after relaxation and computed the ^{17}O NMR parameters on these new coordinates. The total energy increases by 4.47 meV as a result of this exchange. The effect of the exchange is local; i.e., the ^{17}O NMR parameters of the O sites not involved by the Si−Al exchange are not modified. In addition to the calculations on the glass model, we consider an O tricluster in a crystalline environment. Grossite, of composition $CaAl_4O_7$, is the only crystalline system that contains an O tricluster and for which an experimental ^{17}O NMR spectrum is available.[22] In a previous calculation,[21] we have obtained the NMR parameters of the OAl_3 tricluster present in grossite. The theoretical parameters of this tricluster nicely coincide with those measured for one site of grossite, confirming the assignment proposed in ref 22.

Table 1 gives the structural information (T−O distances and T−O−T angles, T = Si, Al) and the corresponding theoretical ^{17}O NMR parameters for all the four O triclusters described above. The structural free parameters, i.e., the angles on the oxygen atom of the triclusters are much less dispersed than those of the Si−O−Si and Si−O−Al sites. Moreover, the two different OAl_3 triclusters present similar NMR parameters. Finally, the Cq and δ values of the OAl_3, OAl_2Si and $OAlSi_2$ sites are very similar to those computed in refs 16 and 17 on small clusters. These three observations suggest that the NMR parameters of each tricluster type are much less dispersed than those of Si−O−Si and Si−O−Al sites. In this case, the NMR parameters presented in Table 1 could be used to identify the NMR signature of each type of tricluster.

The NMR parameters of the four O triclusters are reported in Figures 8 and 9. The NMR parameters of the OAl_2Si and $OAlSi_2$ sites are in the same range covered by the Si−O−Si and the Si−O−Al sites. Since the triclusters are present in the glass in very small quantities, it is very unlikely that ^{17}O NMR could detect this type of site. On the other hand, the NMR parameters of the OAl_3 triclusters are close to the edge of the main Si−O−Al and Al−O−Al peaks and their position is in agreement with the expected position of this tricluster type proposed by Stebbins et al. in ref 22.

The position of our OAl_3 tricluster sites on the 2D-3QMAS spectrum does not exactly coincide with the D peak observed in the experimental spectrum of Stebbins and Zhu measured on a tectosilicate CAS glass[6] but are located at the right edge of this peak. Thus, it is difficult either to confirm or to disprove the attribution of the D peak to O triclusters. Indeed, according to our results, only O triclusters of the OAl_3 type could be attributed to the D peak. Yet this would require that the effect of disorder could shift the positions of these oxygen sites ≈10−20 ppm in the isotropic dimension.

Finally, our results suggest that it is very unlikely that ^{17}O NMR could detect this type of oxygen site and that if the D peak could be attributed to tricluster units, it could only be attributed to the AlO_3 tricluster type.

3.4. ^{17}O Parameters for the CAS Glass: Correlations with Geometry. Another interesting feature of NMR spectroscopy is the possibility to correlate the measured parameters with the local environment, i.e., with the bond lengths, angles, and coordination numbers.

In Figure 10, we present the ^{17}O chemical shift δ and the δ_{3Qiso} value of the NBO atoms as a function of the distance between the NBO and its nearest calcium neighbor Ca*. It is clear that both the ^{17}O chemical shift and the δ_{3Qiso} value strongly depend on the NBO−Ca* distance. Linear fits of the

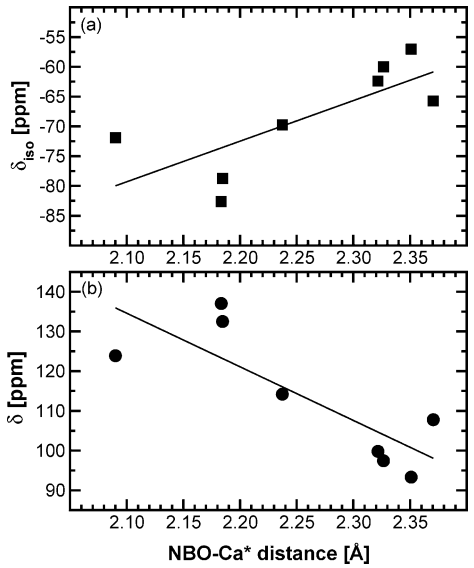

Figure 10. Values of δ^{3Qiso} (upper graph) and the chemical shift δ (lower graph) for each NBO atom as a function of the distance between the NBO atom and its nearest calcium neighbor Ca*.

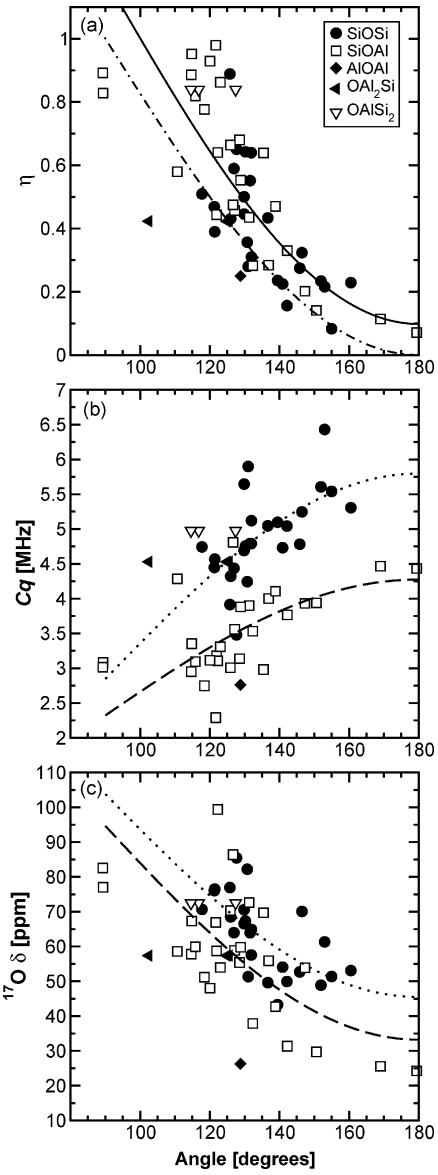

Figure 11. Variation of the calculated ^{17}O NMR (a) asymmetry parameter η, (b) quadrupolar coupling Cq, and (c) chemical shift δ as a function of the corresponding T−O−T angles (T = Si, Al) in the CAS glass. The different symbols denote different O sites. The lines represent fits to the $y = a + b\cos(\theta)$ (θ is the T−O−T angle) function for Si−O−Si sites (dotted line), Si−O−Al sites (dashed line), and Si−O−T (T = Si,Al) sites (bold line). The dot−dashed line is the fit obtained from parameters computed by the authors of ref 67 for SiO_2. The points corresponding to the edge-sharing tetrahedra have not been considered for the fits.

points presented in Figure 10 give the following values for the straight line coefficients: δ_{3Qiso} [ppm] = 68.21 × $d_{NBO-Ca*}$[Å] − 222.56 and δ[ppm] = − 135.09 × $d_{NBO-Ca*}$[Å] + 418.30. Given the sensitivity of the ^{17}O δ_{3Qiso} on the NBO−Ca* distance, the agreement between experimental and theoretical 2D-3QMAS spectra shown in Figure 9 indicates that the NBO−Ca* distances of our glass model reproduce well those from experiment.

From our calculations, we can also extract the variation of the different parameters, namely the chemical shift δ, the quadrupolar coupling Cq and the asymmetry parameter η, as a function of the T−O−T angles (T = Si, Al). The results are presented in Figure 11. For the tricluster O (triangles), three different points corresponding to the three different T−O−T angles are depicted on the graph.

TABLE 2: Parameters of the Fits Applied on the Dependence on the T−O−T Angles for δ, Cq, and η in the CAS Glass Depicted in Figure 10[a]

	δ			Cq		
	a	*b*	*R*	*a*	*b*	*R*
Si−O−Si	58.29	103.80	0.66	−2.950	2.856	0.60
Si−O−Al	61.42	94.65	0.59	−1.952	2.322	0.55

	η		
	a	*b*	*R*
Si−O-[Si,Al]	1.093	1.191	0.72

[a] The fitting function is of the $y = a + b\cos(\theta)$ form, θ being the T−O-T angle and R gives the correlation coefficient of the fit. The points corresponding to the edge-sharing tetrahedra have not been considered for the fits.

In Figure 11c, the chemical shifts are shown as a function of the corresponding T−O−T angles. The chemical shift is weakly correlated with the T−O−T angle, even if it is possible to associate a larger chemical shift with a small T−O−T angle. The best fits of the Si−O−Al and Si−O−Si chemical shift dependence on angle are given in Table 2 and are shown as dashed and dotted lines, respectively. They are obtained using a function of the form $y = a + b\cos(\theta)$, where θ is the T−O−T angle.

In Figure 11b, the calculated quadrupolar couplings Cq in MHz are depicted as a function of the corresponding T−O−T angles for each O atom. As for the chemical shifts, it is difficult to extract a clear dependence of the Cq parameter on the T−O−T angle even if a trend can be seen: the Cq values tend to increase as a function of the angles and to be larger for the Si−O−Si sites than for the Si−O−Al sites. Again, we show the best fits for Si−O−Al and Si−O−Si Cq values separately, in dashed and dotted lines respectively and the fit parameters are reported in Table 2.

A better correlation is found between asymmetry parameter η and the T−O−T angle, as shown in Figure 11a. In this case, the dependence is similar for the Si−O−Al and the Si−O−Si sites, and a single fit is presented in the figure and in Table 2. We also report in Figure 11a the fit proposed by the authors of ref 67 for SiO_2 polymorphs, as a dot−dashed line.

Contrary to our findings, ref 16 shows perfect correlations between the Si−O−Si angles and the chemical shifts and the Cq parameters. According to our results, these perfect correlations appear to be an artifact due to the use of small clusters in ref 16 that are not able to represent the local disorder present in ternary glasses.

4. Conclusion

We have generated a calcium aluminosilicate glass quenched from the melt using ab initio molecular-dynamics simulations of the Car−Parrinello type in which we found an excess number of nonbridging O atoms that are compensated by O triclusters. The local structure of the glass was compared to NMR experiments by computing the ^{17}O NMR parameters and 2D-3QMAS NMR spectrum from first-principles simulations. The computed NMR parameters are in good agreement with those measured by a 2D-3QMAS NMR experiments.

In the computed 2D-3QMAS spectrum of the CAS glass, the OAl_2Si and $OAlSi_2$ tricluster sites are located under the main Si−O−Si peak making their experimental detection impossible. The theoretical NMR parameters of the OAl_3 tricluster sites coincide with the ones obtained for the OAl_3 tricluster site of

the grossite crystal but not with the D peak that is observed in the experimental ^{17}O 2D-3QMAS NMR spectra of a CAS glass.[6]

Finally, correlations of the chemical shifts, the quadrupolar couplings Cq and the asymmetry parameters η with the T−O−T angles in the CAS glass were obtained and fitted to cosine functions. The asymmetry parameter η exhibits a clear correlation with the cosine of the T−O−T angle. A weaker correlation is found for the Cq and the chemical shift.

This work shows that the use of a molecular-dynamics-generated model and of periodic boundary conditions allows to consider the effect of disorder in the simulation of the NMR spectrum and thus to obtain an exceptionally good agreement with experiment. Applications to CAS glasses of different compositions give hope for improved interpretation of the NMR experimental data.

Acknowledgment. We would like to thank Simona Ispas and Walter Kob for constant interesting discussions. The work of CJP was funded by the EPSRC. The calculations have been carried out on IBM SP3 and SP4 in the French computer centers CINES in Montpellier and IDRIS in Orsay.

References and Notes

(1) Bansal, N. P.; Doremus, R. H. *Handbook of Glass Properties*; Academic Press. Inc.: Orlando, FL, 1986.
(2) Muller, E.; Heide, K.; Zanotto, E. D. *J. Non-Cryst. Solids* **1993**, *155*, 56.
(3) Toplis, M. J.; Dingwell, D. B.; Lenci, T. *Geochim. Cosmochim. Acta* **1997**, *61*, 2605.
(4) Tossell, J. A.; Cohen, R. E. *J. Non-Cryst. Solids* **2001**, *286*, 187.
(5) Wu, Z. et al. *Phys. Rev. B* **1999**, *60*, 9216.
(6) Stebbins, J. F.; Xhu, Z. *Nature* **1997**, *390*, 60. Farnan, I. *Nature* **1997**, *390*, 14.
(7) Stebbins, J. F.; Oglesby, J. V.; Lee, S. K. *Chem. Geol.* **2001**, *174*, 63.
(8) Stebbins, J. F.; Kroeker, S.; Lee, S. K.; Kiczenski, T. J. *J. Non-Cryst. Solids* **2000**, *275*, 1.
(9) Stebbins, J. F.; Lee, S. K.; Oglesby, J. V. *Am. Mineral.* **1999**, *84*, 983.
(10) Angeli, F.; Delaye, J.-M.; Charpentier, T.; Petit, J.-C.; Ghaleb, D.; Faucon, P. *Chem. Phys. Lett.* **2000**, *320*, 681.
(11) Baltisberger, J. H.; Xu, Z.; Stebbins, J. F.; Wang, S. H.; Pines, A. *J. Am. Chem. Soc.* **1996**, *118*, 7209.
(12) Poe, B. T.; Romano, C.; Zotov, N.; Cibin, G.; Marcelli, A. *Chem. Geol.* **2001**, *174*, 21.
(13) McManus, J.; Ashbrook, S. E.; MacKenzie, K. J. D.; Wimperis, S. *J. Non-Cryst. Solids* **2001**, *282*, 278.
(14) Lee, S. K.; Stebbins, J. F. *J. Phys. Chem. B* **2000**, *104*, 4091.
(15) Merzbacher, C. I.; Sheriff, B. L.; Hartman, J. S.; White, W. B. *J. Non-Cryst. Solids* **1990**, *124*, 194.
(16) Xue, X.; Kanzaki, M. *J. Phys. Chem. B* **1999**, *103*, 10816.
(17) Kubicki, J. D.; Toplis, M. J. *Am. Mineral.* **2002**, *87*, 668.
(18) Pickard, C. J.; Mauri, F. *Phys. Rev. B* **2001**, *63*, 245101.
(19) Profeta, M.; Mauri, F.; Pickard, C. J. *J. Am. Chem. Soc.* **2003**, *125*, 541.
(20) Blöchl, P. E. *Phys. Rev. B* **1994**, *50*, 17953.
(21) Profeta, M.; Mauri, F.; Benoit, M.; Pickard, C. J. *J. Am. Chem. Soc.* **2004**, *126*, 12528.
(22) Stebbins, J. F.; Oglesby, J. V.; Kroeker, S. *Am. Mineral.* **2001**, *86*, 1307.
(23) Mueller, K. T.; Baltisberger, J. H.; Wooten, E. W.; Pines, A. *J. Phys. Chem.* **1992**, *96*, 7001.
(24) Car, R.; Parrinello, M. *Phys. Rev. Lett.* **1985**, *55*, 2471.
(25) Benoit, M.; Ispas, S.; Tuckerman, M. E. *Phys. Rev. B* **2001**, *64*, 224205.
(26) CPMD Version 3.3, Hutter, J.; Alavi, A.; Deutsch, T.; Bernasconi, M.; Goedecker, St.; Marx, D.; Tuckerman, M.; Parrinello, M. MPI für Festkörperforschung and IBM Research (1995−1999).
(27) Kohn, W.; Sham, L. *Phys. Rev.* **1965**, *140 A*, 1133.
(28) Becke, A. D. *Phys. Rev. A* **1988**, *38*, 3098.
(29) Lee, C.; Yang, W.; Parr, R. G. *Phys. Rev. B* **1988**, *37*, 785.
(30) Trouiller, N.; Martins, J. *Phys. Rev. B* **1991**, *43*, 1993.
(31) GÃ¶decker, S.; Teter, M.; Hutter, J. *Phys. Rev. B* **1996**, *54*, 1703.
(32) Martyna, G. J.; Tuckerman, M. E.; Klein, M. L. *J. Chem. Phys.* **1992**, *97*, 2635.
(33) Tuckerman, M. E.; Parrinello, M. *J. Chem. Phys.* **1994**, *101*, 1302.
(34) Huang, C.; Behrman, E. C. *J. Non-Cryst. Solids* **1991**, *128*, 310.
(35) Vollmayr, K.; Kob, W.; Binder, K. *Phys. Rev. B* **1996**, *54*, 15808 and references therein.
(36) www.ncnr.nist.gov/resources/n-lenths/elements/.
(37) Cormier, L.; Neuville, D. R. Private communication.
(38) Ganster, P.; Benoit, M.; Kob, W.; Delaye, J.-M. *J. Chem. Phys.* **2004**, *120*, 10172.
(39) Ganster, P. Ph.D. Thesis, Université Montpellier II, France 2004.
(40) Brown, G. E.; Gibbs, G. V.; Ribbe, P. H. *Am. Mineral.* **1969**, *54*, 1044.
(41) Taylor, M.; Brown, G. E. *Geochim. Cosmochim. Acta* **1979**, *43*, 61.
(42) Gibbs, G. V.; Meagher, E. P.; Newton, M. D.; Swanson, D. K. *In: Structure and Bonding in Crystals I*; O'Keeffe, M., Navrotsky, A., Eds.; Academic Press: New York, 1981; p 195.
(43) Navrotsky, A.; Geisinger, K. L.; McMillan, P.; Gibbs, G. V. *Phys. Chem. Miner.* **1985**, *11*, 284; Brown, G. E.; Farges, F.; Calas, G. In: Structure, Dynamics and Properties of Silicate Melts, Ed: Stebbins, J. F.; McMillan, P. F.; Dingwell, D. B. *Rev.. Miner.* **1995**, 32.
(44) Himmel, B.; Weigelt, J.; Gerber, Th.; Nofz, M. *J. Non-Cryst. Solids* **1991**, *136*, 27.
(45) Petkov, V.; Gerber, Th; Himmel, B. *Phys. Rev. B* **1998**, *58*, 11982.
(46) Petkov, V.; Billinger, S. J. L.; Shastri, S. D.; Himmel, B. *Phys. Rev. Lett.* **2000**, *85*, 3436.
(47) Stebbins, J. F. *Nature* **1987**, *330*, 13.
(48) Lee, S. K.; Stebbins, J. F. *Am. Mineral.* **1999**, *84*, 937.
(49) Lee, S. K.; Stebbins, J. *J. Phys. Chem.* **2000**, *104*, 4091.
(50) Myers, E. R.; Heine, V.; Dove, M. T. *Phys. Chem. Miner.* **1998**, *25*, 457.
(51) Tossel, J. A. *Am. Mineral.* **1993**, *78*, 911.
(52) Cormier, L.; Neuville, D. R.; Calas, G. *J. Non-Cryst. Solids* **2000**, *274*, 110.
(53) Benoit, M.; Ispas, S.; Jund, P.; Jullien, R. *Eur. Phys. J. B* **2000**, *13*, 631.
(54) Mauri, F.; Pasquarello, A.; Pfrommer, B. G.; Yoon, Y.-G.; Louie, S. G. *Phys. Rev. B* **2000**, *62*, R4786.
(55) Yuan, X.; Cormack, A. N. *J. Non-Cryst. Solids* **2003**, *319*, 31.
(56) Pasquarello, A.; Car, R. *Phys. Rev. Lett.* **1998**, *80*, 5145.
(57) Rahmani, A.; Benoit, M.; Benoit, C. *Phys. Rev. B* **2003**, *68*, 184202.
(58) Winkler, A.; Horbach, J.; Kob, W.; Binder, K. *J. Chem. Phys.* **2003**, *120*, 384.
(59) Troulier, N.; Martins, J. L. *Phys. Rev. B* **1991**, *43*, 1993.
(60) Kleinman, L.; Bylander, D. *Phys. Rev. Lett.* **1982**, *48*, 1425.
(61) Baldereschi, A. *Phy. Rev. B* **1973**, *7*, 5212.
(62) Petrilli, H. M.; Blöchl, P. E.; Blaha, P.; Schwarz, K. *Phys. Rev. B* **1998**, *57*, 14690.
(63) Perdew, J. P.; Burke, K.; Ernzerhof, M. *Phys. Rev. Lett.* **1996**, *77*, 3865.
(64) Perdew, J. P.; Wang, Y. *Phys. Rev. B* **1986**, *33*, 8800. Perdew, J. P.; *Electronic Structure of Solids*; Ziesche, P.; Eschrig, H., Eds.; Academic: Berlin, 1991.
(65) Stebbins, J. F.; et al. *Solid State NMR* **1997**, *8*, 1.
(66) Stebbins, J. F.; Oglesby, J. V.; Xu, Z. *Am. Mineral.* **1997**, *82*, 1116.
(67) Tossell, J. A.; Lazzeretti, P. *Phys. Chem. Miner.* **1988**, *15*, 564.